

# Vertical Electrical Sounding Technique for Assessing the Quaternary Aquifer Vulnerability to Contamination in the Semi-Arid Khanasser Valley Region, Northern Syria

**Jamal Asfahani**

Atomic Energy Commission

Geology Department

P.O. Box. 6091, Damascus- Syria

Email: ([cscientific@aec.org.sy](mailto:cscientific@aec.org.sy)) < Jamal Asfahani)

<https://orcid.org/0000-0002-9302-9771>

## Abstract

The aim of this paper is to evaluate the vulnerability of groundwater to contamination by adapting aquifer vulnerability index (*AVI*) approach, based mainly on the hydraulic conductivity (*K*) of the aquifer and overburden layers' thickness (*h*). The *technique* of vertical electrical sounding (*VES*) with the configuration of Schlumberger was applied to model the Quaternary aquifer and its overburden layers in the Khanasser Valley area in Northern Syria. According to *AVI* classification, 5.88% of the study area is hugely polluted, 67.00% highly polluted, 23.53% moderately polluted, and 2.94% lowly polluted. Several hydro-geochemical parameters which affect the Aquifer Vulnerability Index (*AVI*) (such as anisotropy ( $\lambda$ ) of the subsurface hydrogeological layers, thickness (*hOverb*), resistivity ( $\rho_{Overb}$ ), hydraulic conductivity (*K*), and hydraulic resistance (*C*) of the protecting layers) are statistically analyzed. Different mutual empirical relationships between the above parameters are established through analyzing their statistical correlation matrix. The derived empirical relationships highlight the mutual hydrological processes and the lithological connectivity nature between the study Quaternary aquifer and its overlaying layers. The obtained results highlighted the importance of safeguarding groundwater resources, and outlined resource allocation to protect the aquifer zones, for decision-makers. This was the first time that *AVI* approach is applied in Syria, and can be consequently extended to other Syrian aquifers. *AVI* can be also applied worldwide to estimate the conditions dominating the aquifer's protectivity in semi-arid regions.

**Keywords:** aquifer vulnerability index, hydraulic conductivity, hydraulic resistance, Semi-arid Khanasser valley, Syria.

## 1. Introduction

The contaminations originating from the surface affect the groundwater stored in the aquifers (Ikpe et al., 2021). The anthropogenic activities negatively affect the groundwater quality due to poor waste disposal management, the leakages from the surface and underground storage tanks, mining activities, and latrines, sewage from oil spillage, and the movement of leachates from dumpsites into subsurface hydrogeological units (Oseji et al. 2018).

The hydrogeological aquifer systems are well protected from surface contamination and pollution when the overlaying earth layers above an aquifer have suitable hydrological conditions, regarding their resistivities, thicknesses, and hydraulic conductivities.

The aquifer overburden layers act as natural boundaries to filter percolating surface contaminated fluids, and the measure of such an ability determines the aquifer protectivity characteristics (Adeniji et al. 2014).

The protectivity of the underlying hydrogeological aquifer is considerably affected by some critical factors, which are the thickness, porosity, grain size, hydraulic conductivity, and anisotropy of the overburden-protecting layers (Mogaji et al., 2011; Adeniji et al. 2014; Ekanem, 2020; Ekanem et al. 2020; Ikpe et al., 2022; Asfahani, 2023a; Asfahani 2023b).

The high resistivity and high hydraulic conductivity of the permeable overlaying layers of sand and gravel facilitate the easy movement of the surface fluid contaminants and their infiltration into the aquifer system. On the contrary, the low hydraulic conductivity and low resistivity of the impervious overburden layers of clay and shale retard and slow the infiltration rate of the surface contaminants into the subsurface, such as the protectivity of the aquifer is improved considerably (Adeniji et al. 2014; Ayuk 2019; Ekanem et al. 2021; Asfahani 2023a; Asfahani 2023b).

Electrical resistivity technology, with its different approaches and different configurations, particularly the (*VES*) one, has been largely practiced in solving and characterizing different groundwater and hydrological problems related to aquifer potentiality, and contamination, by locating vulnerable zones, migration and the extent of contamination (Ebong et al., 2014; Obiora et al., 2016; Laouini et al, 2017;

Eyankware, 2019; Oli et al., 2020; Ekwe et al., 2020; Eyankware et al. 2020a, b, & 2021; Eyankware et al., 2022).

The aquifer vulnerability conditions of a given region can be easily determined by using the vertical sounding technique (*VES*), and the fast and simple aquifer vulnerability index *AVI* approach (Stempvoort et al., 1993; Obiora and Ibuot, 2020; Ossai et al., 2020).

The conductivity of the most contaminants is much higher than the conductivity of natural groundwater, where such pronounced conductivity contrast enables an easy identification of contamination plumes by using geoelectrical methods, particularly the *VES* one. The *VES* technique can be used to describe the aquifer hydrogeological units in detail and detect their contaminant plume.

The overburden-protective capacity of an aquifer is controlled by several geoelectrical parameters, which are the resistivity ( $\rho_{Over}$ ), thickness ( $h_{Over}$ ), the anisotropy of the subsurface hydrogeological layers ( $\lambda$ ), and the hydraulic conductivity ( $K$ ) of the overburden layers.

The modeling of the influence of those parameters through analyzing their quantitative results by the *AVI* approach allow us to characterize and describe the protected aquifer areas and determine the contamination conditions surrounding the study aquifer. The mutual hydrological processes and the lithological connectivity between the studied aquifer and its overlaying layers can be quantitatively estimated by developing and establishing specific empirical relationships between the different related hydro-geophysical parameters.

The direct focus on determining the protectivity conditions and the contamination of the Quaternary aquifer in the semi-arid Khanasser Valley region, Northern Syria is the originality of this work through the application of both the *VES* technique and the aquifer vulnerability index *AVI* method.

The quantitative modeling of *VES* and *AVI* results allows determining the hydrogeological connectivity conditions between the Quaternary aquifer and its overlaying layers. The different geoelectrical parameters affecting the aquifer protectivity and its contamination are discussed, documented, and compared with other new geoelectrical contamination approaches (Asfahani 2023a; Asfahani 2023b). The new geoelectrical research works oriented towards determining the protectivity

and the contamination of the aquifers, recently carried out, are undertaken in Syria for the first time (Asfahani 2023a; Asfahani 2023b).

The main goals of this research are therefore the following:

- 1- To apply the integrated electrical resistivity (*VES*) technique and the *AVI* approach to estimate the Quaternary aquifer susceptibility to surface contamination, and to locate the possible contaminated vulnerable zones in the study area;
- 2- To analyze the different geoelectrical parameters influencing and affecting the vulnerability to contamination conditions, by applying the statistical correlation matrix;
- 3- To follow the different spatial variations of those parameters in the study region;
- 4- To derive different empirical equations between the analyzed parameters in 2.

## **2. Hydrogeology of the Khanasser Valley**

Khanasser Valley region is one of the integrated research sites of the International Center for Agriculture in Arid Dry Areas (ICARDA) National Resource Management Program. The choice of this site location was oriented basically towards addressing the different problems related to the marginal dryland environments. The dynamics and diversity of the natural resources and livelihoods, poverty, and the relatively easy accessibility to the study area make the Khanasser region a prime preferable candidate (Asfahani, 2007). The vulnerability to contaminations in the semi-arid regions is an important critical matter, where the geoelectrical researches are mainly concentrated on locating the areas of acceptable contamination ranges for fresh, drinkable groundwater sites.

Khanasser Valley is located approximately 70 km southeast of Aleppo City (Fig.1), and situated between two hills, Jabal Al Hoss in the west and Jabal Shbeith in the east. The drain of the northern and southern parts of the valley is towards Jaboul salt lake and the Adami depression respectively, as indicated by . Figs (1 and 2).

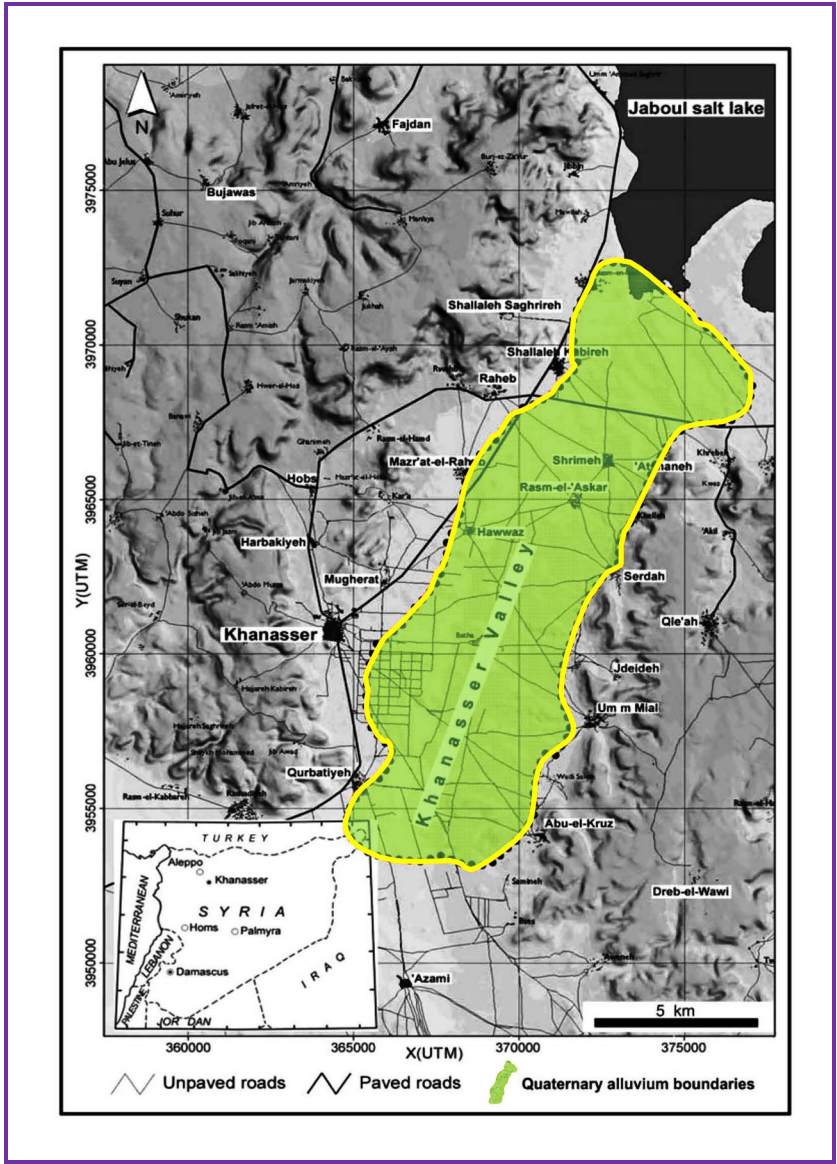
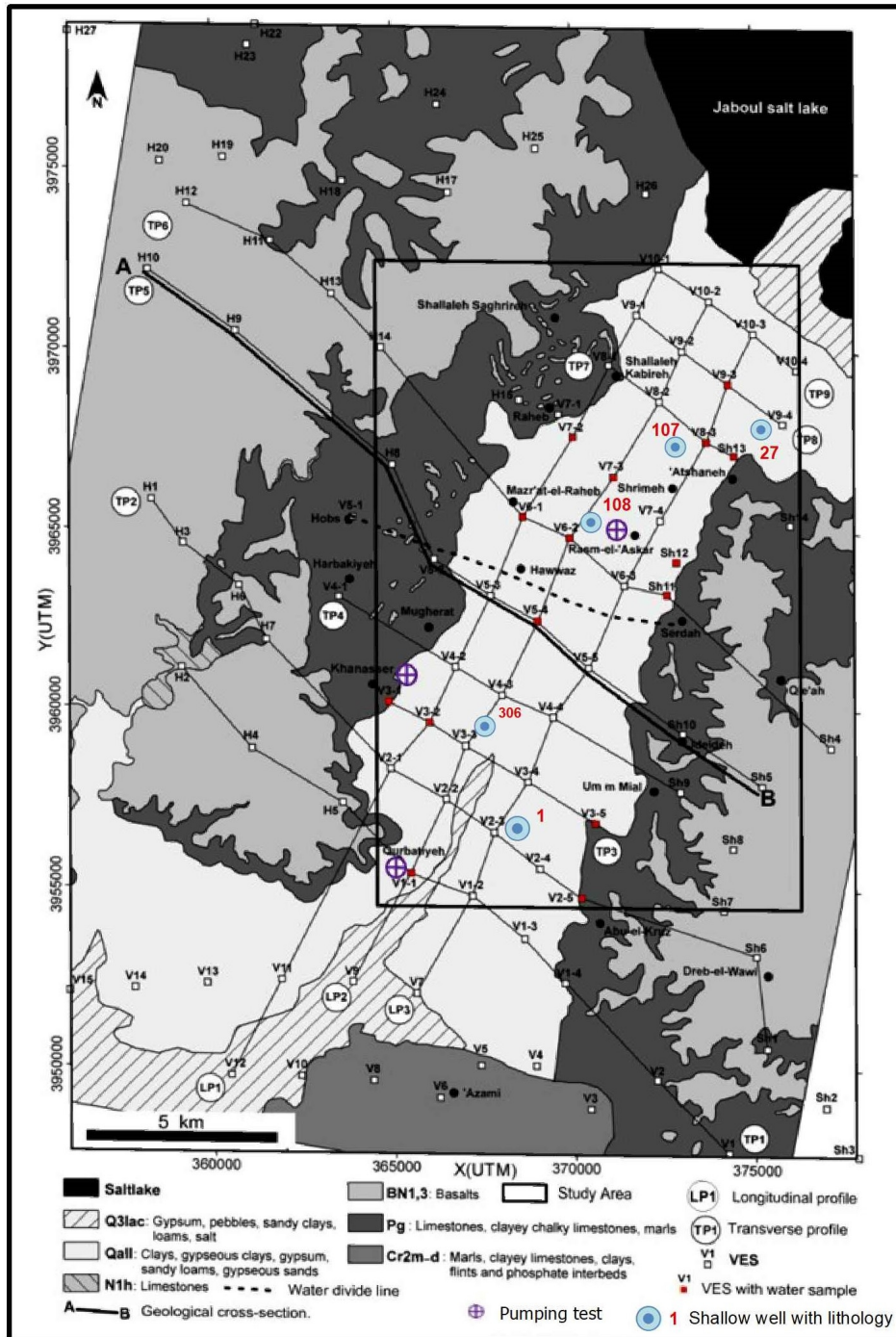


Figure 1. Location of the Khanasser Valley study region, Northern Syria.



**Figure 2.** The *VES* points locations, on the geological map of the Khanasser Valley and its surroundings (After Ponikarov, 1964).

Three aquifers exist in the semi-Khanasser Valley region to extract groundwater. The deepest one related to the upper Cretaceous is 400 m under the ground level. Low-productive aquifer of Paleocene-Lower Eocene limestone is found above the

Maestrichtian (ACSAD, 1984). The average hydraulic conductivity ( $k$ ) of this aquifer is equal to 0.0054 m/day (Schweers et al., 2002). The Paleogene strata of about 50 m of Paleocene and lower Eocene in the central part of the Khanasser valley are not sufficiently thick over the Maestrichtian formation. The Quaternary aquifer, located near the surface and covered by the alluvial and colluvial sediments of about 10 m is the most transmissive hydrological structure in the study area.

The rainwater, the infiltrating runoff, and the subsurface flow from the Jabal Shbeith and Jabal Al Hoss slopes provide the direct recharge for this aquifer.

### 3. Methodology

#### 3.1. VES technique

The electrical resistivity sounding technique is applied to measure the subsurface resistivity distribution in the study Khanasser region, Northern Syria. Thirty-four (34) vertical electrical soundings (VES) points are measured by using Schlumberger electrode array.

The electrical current ( $I$ ) is injected into the earth by two electrodes ( $A$  and  $B$ ), while the generated potential differences ( $\Delta V$ ) is measured by two potential electrodes ( $M$  and  $N$ ) as indicated by Fig.3-a.

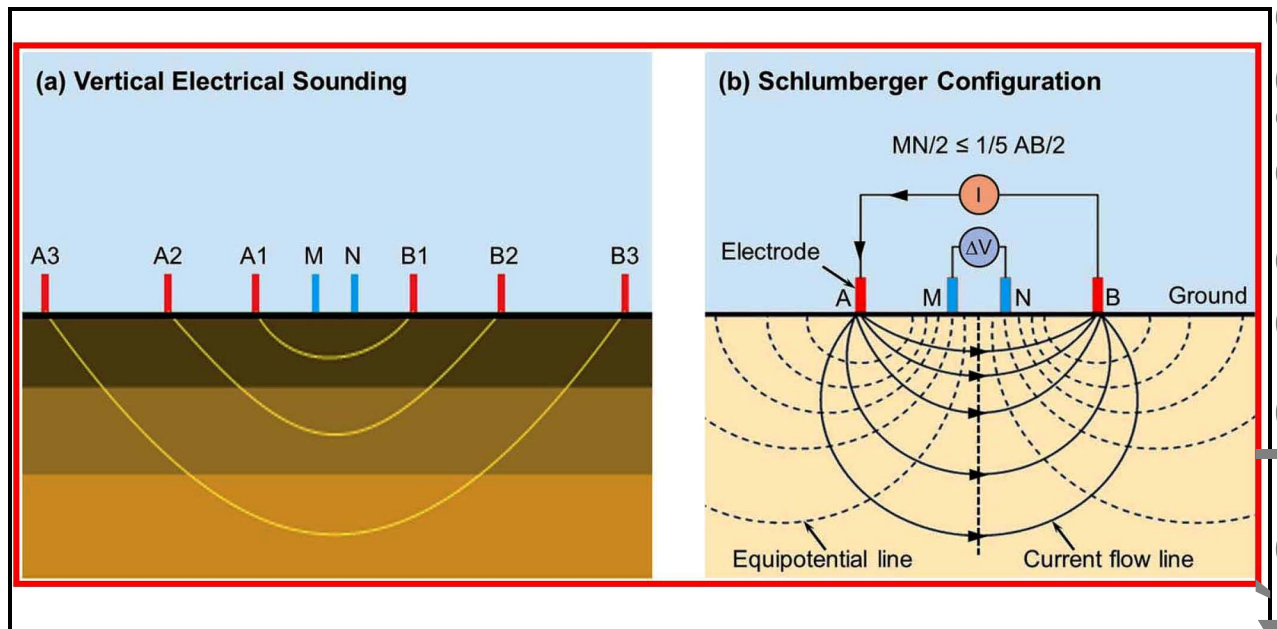


**Figure 3 (a).** VES Schlumberger configuration and its field operation in the field (Othman et al., 2022).

The Indian resistivity meter (*DDRI*) directly measures the apparent resistance ( $\Delta V/I$ ) of the layers the electrical current penetrates. The apparent resistivity was thereafter evaluated through using the following equation (Dobrin, 1988):

$$\rho_a = \frac{2\pi}{\frac{1}{AM} - \frac{1}{BM} - \frac{1}{AN} + \frac{1}{BN}} \frac{\Delta V}{I} \quad (1)$$

The half-current electrode spacing  $AB/2$  are between 3.0 and 500 m, and the half-potential electrode spacing  $MN/2$  are between 0.25 and 20 m. The increasing of the electrode spacing  $AB/2$  about a fixed point allows the establishment of the complete field apparent resistivity curve in this point ( $\rho_a = f(AB/2)$ ). The field apparent resistivity curve is thereafter quantitatively interpreted by the inversion WINRESIST software of Velpen 2004 in order to obtain the final *ID* corrected optimum model, which verifies as well the goodness of fit between the field resistivity curve and the final theoretical regenerated model (Zohdy, 1989; Zohdy and Bisdorf, 1989).

Figure. 3-b shows the field work during *VES* measurements in the Khanasser Valley region.



**Figure 3 (b).** Field *VES* technique.

Figure 4-a indicates the snapshot WINRESIST for evaluating the theoretical inverted model, while Fig. 4-b indicates the final corresponding *VES* resist graph display.



**Figure 4(a).** A snapshot WINRESIST window during its running . **(b)** Final *VES* resist graph display.

The final optimized model includes the depth, thickness and actual resistivity of the traversed layers under the study *VES* point.

The two fundamental first-order geo-electric indices parameters of layer thickness ( $h$ ) and resistivity ( $\rho$ ) are used for interpreting the geoelectrical models to characterize the stratified subsurface lithological units under each studied *VES* location. The computation of both the hydraulic conductivity ( $K$ ) and the hydraulic resistance ( $C$ ) of the aquifer overburden layers are based on using ( $h$ ) and ( $\rho$ ).

### 3.2. Hydraulic conductivity ( $K$ )

The behavior of the vulnerability overburden protective layers and their hydraulic conductivities are assessed by using the following empirical equation, already proposed and applied for characterizing the alluvial aquifer in the Saharanpur area of India (Singh, 2005):

$$K = 0.0002 * e^{0.0897 * \rho} \quad (2)$$

where  $K$  (m/day) is the hydraulic conductivity and  $\rho$  ( $\Omega.m$ ) is the overburden aquifer resistivity layer. This hydraulic conductivity parameter describes the groundwater movements through the porous and fractured nature of the subsurface alluvial rocks in the study area.

#### 4. Aquifer vulnerability index (AVI)

The AVI approach, proposed by Stempvoort et al. (1993), is used herein to characterize and compute the overburden aquifer vulnerability's hydraulic resistance (C). The parameter (C) expressed in days is evaluated through the parameters of vertical hydraulic conductivity K (m/day) and thickness h (m) of the layers overlaying the aquifer layer as follows (Stempvoort et al., 1993):

$$C = \sum_{i=1}^n \frac{h_i}{K_i} = \frac{h_1}{K_1} + \frac{h_2}{K_2} + \dots + \frac{h_n}{K_n} \quad (3)$$

where  $h_i$  is thickness and  $K_i$  is the hydraulic conductivity of each covering layer.

The logarithm of the hydraulic resistance ( $\log C$ ) is also evaluated to measure the AVI of the overburden layers to the vertical flow of fluid, which expresses the average travel time of a contaminant from the surface to the subsurface aquifer. The relationship between the hydraulic resistance (C) and AVI is shown in Table 1 according to Stempvoort et al. (1993).

**Table 1.** Standard values for  $\log C$  and AVI ratings (Stempvoort et al., 1993).

Hydraulic Resistance C (day)	Log C (day)	Vulnerability (AVI)
0-10	<1	Extremely high
10-100	1-2	High
100-1000	2-3	Moderate
1000- 10000	3-4	Low
> 10000	>4	Extremely low

#### 5. Results and discussion

The inversion WINRESIST software of Velpen 2004 is used to quantitatively interpret the thirty-four field apparent resistivity curves (VES) points in the Khanasser study region. The available lithological description of well No. 306 located close to V3-3 point of QH geoelectrical curve type, with its quantitative interpretation (ID) is shown in Fig.5.

The Rammel Aswad, composed of alluvial gravels and sand is the source of the shallow Quaternary aquifer in the study region, where its high thickness gives high

transmissivity and yields. The brutal changes of Rammel Aswad are responsible on the brutal variation in productivity and yields of wells vertically and laterally, from place to place even in very short distances (Asfahani, 2016).

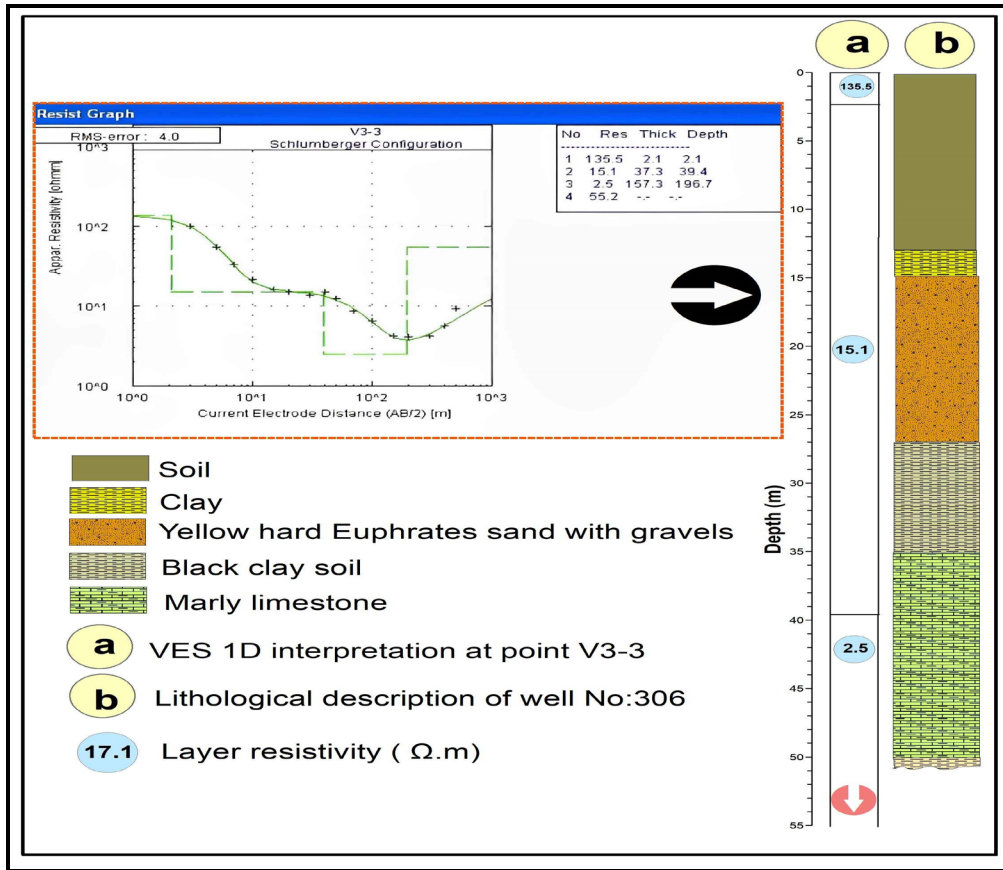


**Figure 5.** Lithology description of Well No: 306 with quantitative *VES* interpretation of *V3-3* point

The *VES* locations with high overburden thickness indicate areas of high protective capacity. The equivalent averaged overburden thickness (*hoverb*) ranges between 1.1m and 28.9m, with an average of 5.33m, as shown in Fig.6.

The equivalent averaged overburden resistivity ( $\rho_{verb}$ ) in the study region ranges between 1.5  $\Omega.m$  and 539  $\Omega.m$  with an average of 64  $\Omega.m$  as indicated in Fig.7.

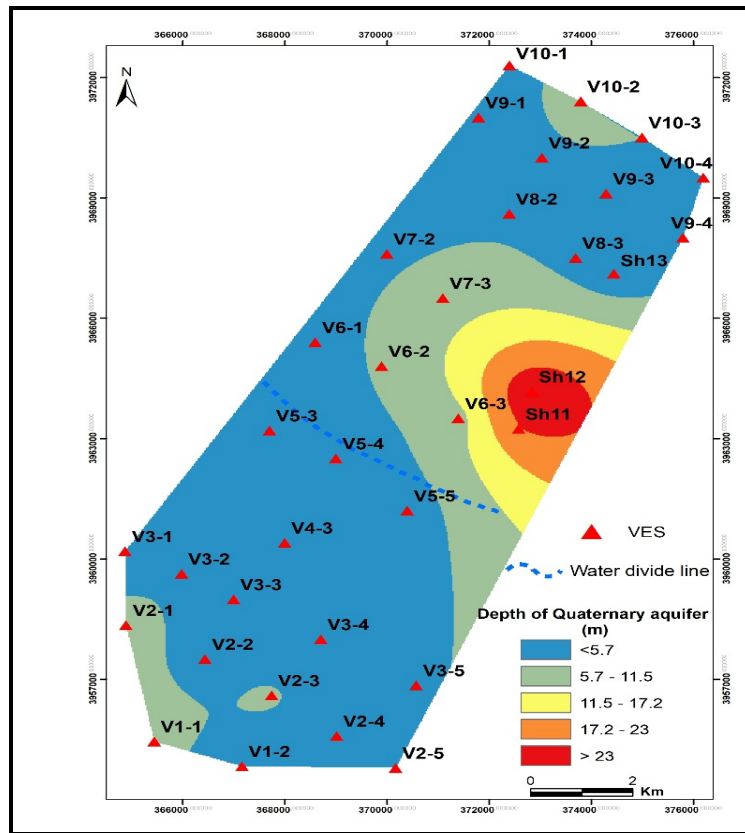


**Figure 6.** Quaternary aquifer overburden thickness of in the Khanasser valley region (Asfahani, 2023a).

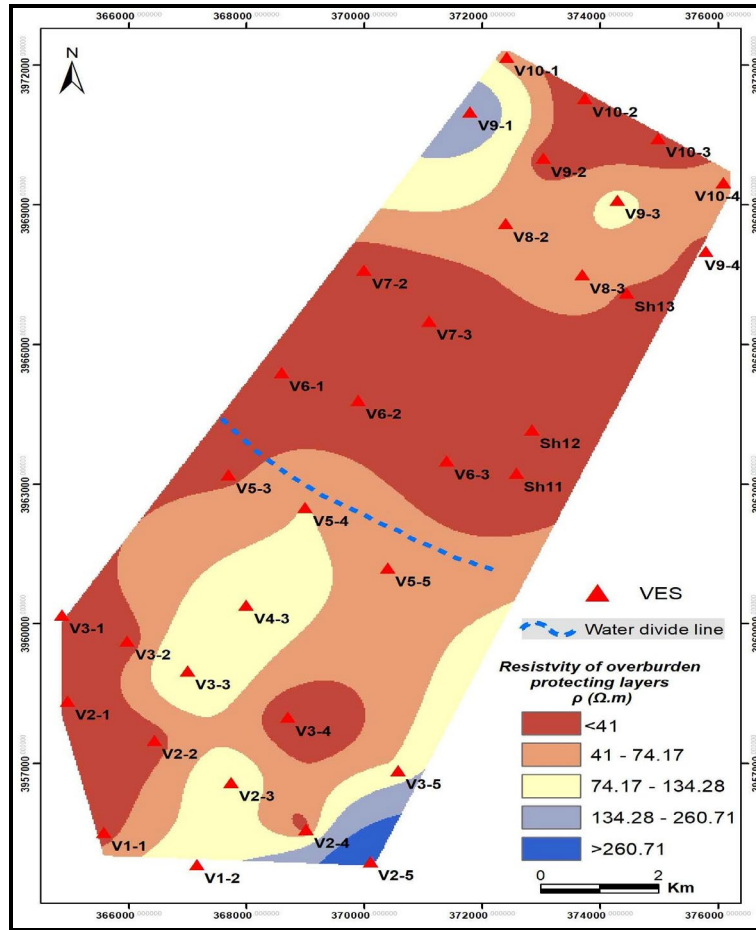


**Figure 7.** Quaternary aquifer overburden resistivity of in the Khanasser valley region.

Equation 2 is used to compute the hydraulic conductivity ( $K$ ) of the overburden layers, where its variation ranges between 0.002 m/day and 32.64 m/day with an average of 1.59 m/day (Table 3). The spatial variations of the ( $K$ ) in the study region are shown in Fig.8.

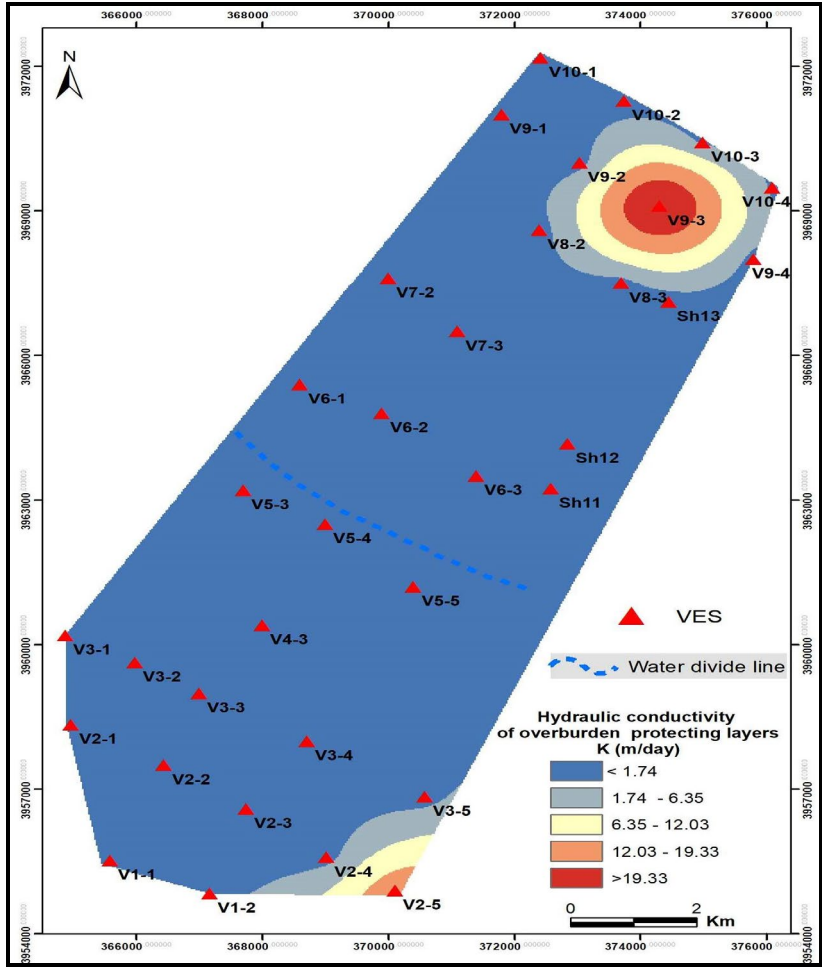


**Figure 8.** Hydraulic conductivity ( $K$ ) of the overburden protecting layers of the aquifer Quaternary in the Khanasser valley region.

The hydraulic resistance ( $C$ ), considered as the most critical parameter in quantifying groundwater vulnerability, is computed according to equation 3. It is based on the thickness and hydraulic conductivity of the layers above the Quaternary aquifer in the study Khanasser area.  $C$  varies between 0.55 and 1659.59 days with an average of 146.68 days (Table 3). The  $\log C$  ranges between -0.26 and 3.22 days with an average of 0.63 days (Table 3). The  $\log C$  variation with the  $VES$  locations is shown in Fig.9, while its spatial variations in the study region are shown in Fig. 10. The capacity of the overburden alluvial rocks to retard and prevent fluid infiltration into the subsurface aquifer is a good indication of its protective capacity.

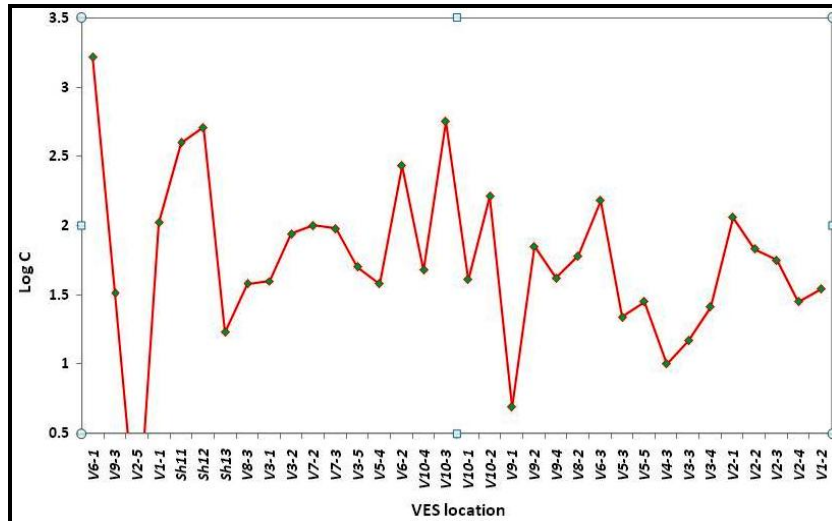


**Figure 9.** Variation of Log C with the thirty-four VES location points in the study area.

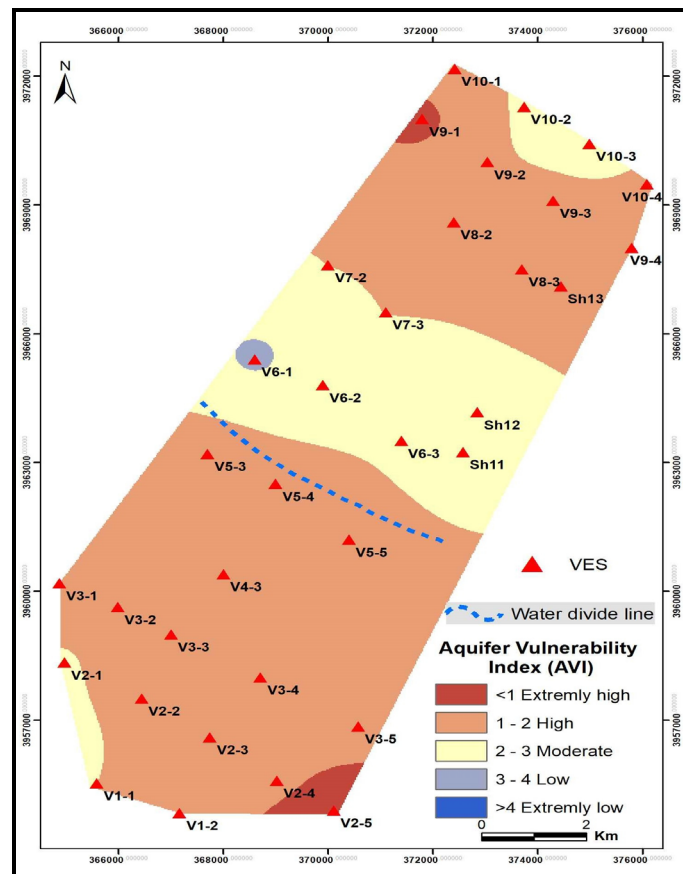


**Figure 10.** Spatial variations of AVI in the study Khanasser region.

The influences of the two thickness (*hoverb*) and resistivity (*ρoverb*) parameters on the Log C are shown in Fig. 11 (a, and b), where two empirical relationships are

established between the  $\text{Log } C$  and  $h_{\text{overb}}$ ,  $\rho_{\text{overb}}$  of the aquifer Quaternary as follows:

$$\text{Log } C = 0.513 \cdot \ln(h_{\text{overb}}) + 0.921 \quad (R^2 = 0.519) \quad (4)$$

$$\text{Log } C = -0.40 \ln(\rho) + 3.181 \quad (R^2 = 0.530) \quad (5)$$

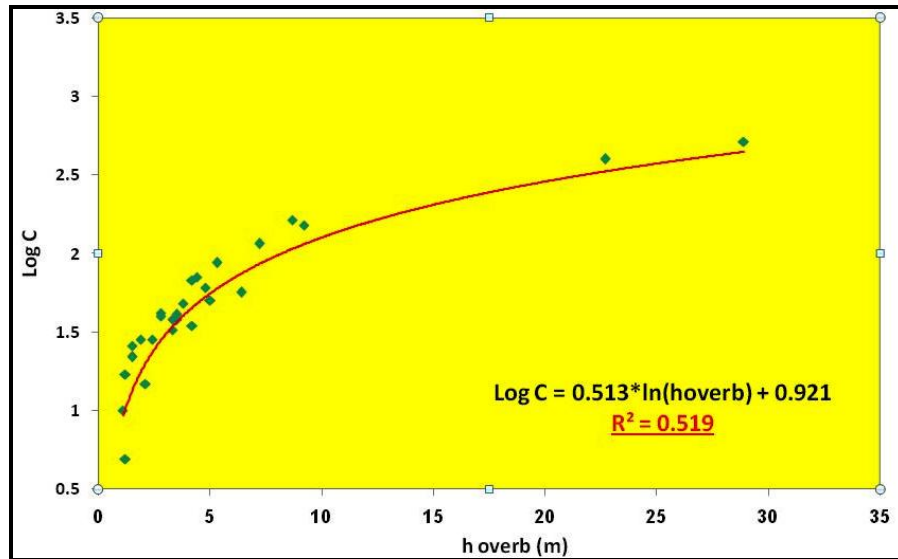


**Figure 11(a).** The empirical relationship between  $\text{Log } C$  and  $(h_{\text{overb}})$  in the study area.

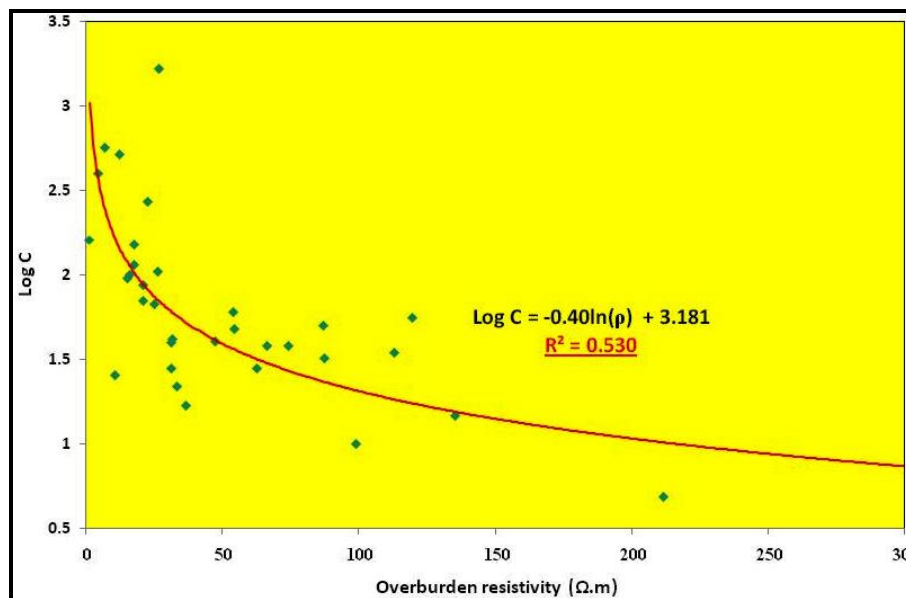


**Figure 11(b).** The empirical relationship between  $\text{Log } C$  and  $(\rho_{\text{overb}})$  resistivity in the study region.

The variations of  $\text{Log } C$  with the hydraulic conductivity ( $K$ ) of the overburden layers are shown in Fig.12, where a decreasing tendency is obtained between them, as much  $K$  is bigger, as much  $\text{Log } C$  is more minor.

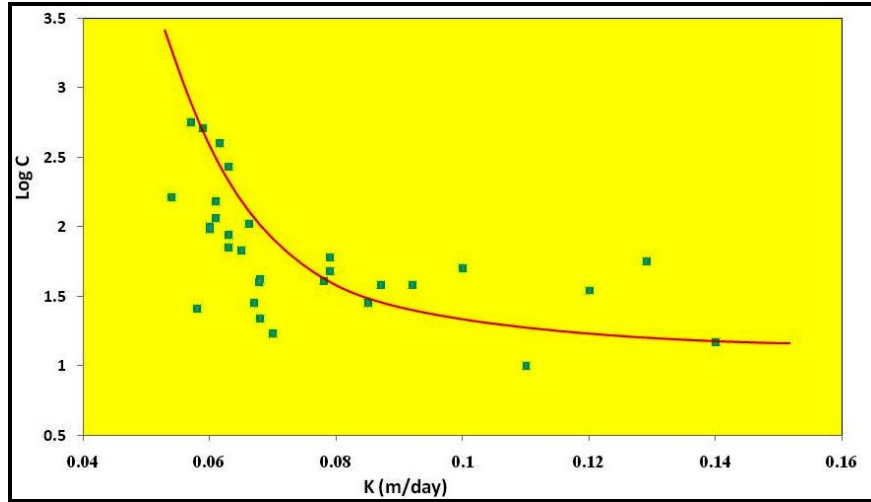


**Figure 12.** Variations of  $\log C$  with  $K$  parameter in the study region.

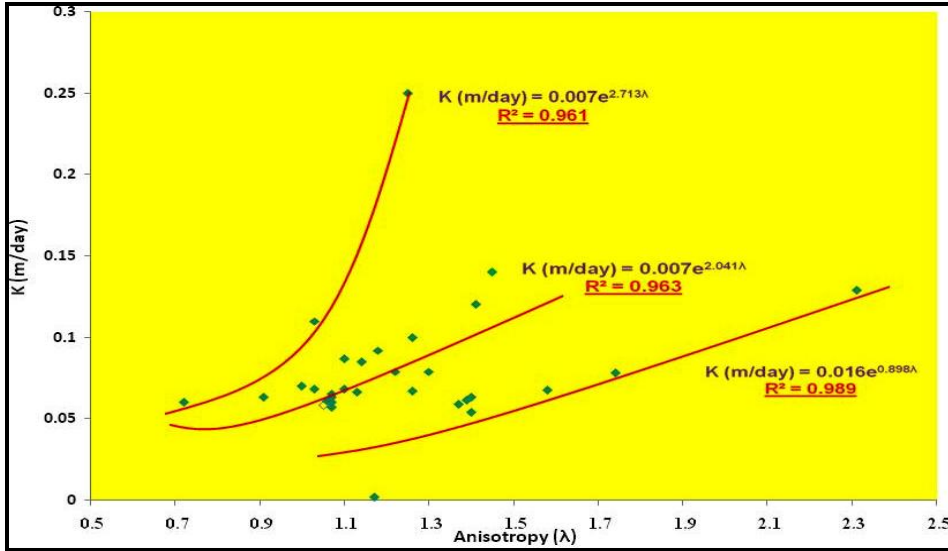
The hydraulic conductivity ( $K$ ) of the overburden layers is related to the anisotropy of the study region (Asfahani, 2023a; Asfahani, 2023b), as attested by Fig.13.

Fig.13 indicates three trends between  $K$  and  $\lambda$ , that reflect different hydraulic systems in the study area. Those exponential trends are quantified by the following three regression equations:

$$K \text{ (m/day)} = 0.007e^{2.713\lambda} \quad (R^2 = 0.961) \quad (6)$$

$$K \text{ (m/day)} = 0.007e^{2.041\lambda} \quad (R^2 = 0.963) \quad (7)$$

$$K \text{ (m/day)} = 0.016e^{0.898\lambda} \quad (R^2 = 0.99) \quad (8)$$



**Figure 13.** Different relationship trends between anisotropy ( $\lambda$ ) and hydraulic conductivity ( $K$ ) in the study area.

The variations of  $h_{Over}$ ,  $\rho_{Over}$ ,  $K$ ,  $C$ ,  $Log C$ ,  $\lambda$ , and  $OPC$  for the measured thirty-four  $VES$  points are shown in Table 2.

**Table 2.** Values of geoelectrical, hydrological, and vulnerability parameters for the measured thirty-four  $VES$  points.

<i>VES Location</i>	$\rho_{Over}$	$h_{Over}$	$K$	$C$	$Log C$	$\lambda$	$OPC$
V6-1	26.8	3.7	0.002	1659.59	3.22	1.17	0.14
V9-3	87.6	3.3	32.64	32.3594	1.51	1.12	0.037
V2-5	539	3.9	18.93	0.54954	-0.26	1.85	0.012
V1-1	26.4		0.0662	104.713	2.02	1.13	-
Sh11	4.8	22.7	0.0616	398.107	2.6	1.39	3.26
Sh12	12.5	28.9	0.0589	512.861	2.71	1.37	4.57
Sh13	36.7	1.2	0.07	16.9824	1.23	1	0.033
V8-3	66.5	3.3	0.087	38.0189	1.58	1.1	0.05
V3-1	31.5	2.8	0.0678	39.8107	1.6	1.58	0.09
V3-2	21.1	5.3	0.063	87.0964	1.94	0.91	0.6
V7-2	16		0.06	100	2	1.07	0.37

V7-3	15.4		0.06	95.4993	1.98	0.72	0.37
V3-5	87	5	0.1	50.1187	1.7	1.26	0.057
V5-4	74.4	<b>3.5</b>	<b>0.092</b>	<b>38.0189</b>	<b>1.58</b>	<b>1.18</b>	<b>0.047</b>
V6-2	22.6		0.063	269.153	2.43	1.07	0.76
V10-4	54.5	3.8	0.079	47.863	1.68	1.22	0.07
V10-3	7.2		0.057	562.341	2.75	1.07	2.5
V10-1	47.45	3.5	0.078	40.738	1.61	1.74	0.094
V10-2	1.5	8.7	0.054	162.181	2.21	1.4	13.75
V9-1	212	1.2	0.25	4.89779	0.69	1.25	0.006
V9-2	21	4.4	0.063	70.7946	1.85	1.4	0.21
V9-4	31.7	2.8	0.068	41.6869	1.62	1.1	0.09
V8-2	54	4.8	0.079	60.256	1.78	1.3	0.09
V6-3	18	9.2	0.061	151.356	2.18	1.06	1.29
V5-3	33.5	1.5	0.068	21.8776	1.34	1.03	0.045
V5-5	63	2.4	0.085	28.1838	1.45	1.14	0.04
V4-3	99	1.1	0.11	10	1	1.03	0.01
V3-3	135.5	2.1	0.14	14.7911	1.17	1.45	0.015
V3-4	10.8	1.5	0.058	25.704	1.41	1.05	0.14
V2-1	18	7.2	0.061	114.815	2.06	1.06	0.49
V2-2	25.4	4.2	0.065	67.6083	1.83	1.07	0.23
V2-3	119.6	6.4	0.129	56.2341	1.75	2.31	0.061
V2-4	31.5	1.9	0.067	28.1838	1.45	1.26	0.06
V1-2	113	4.2	0.12	34.6737	1.54	1.41	0.04

Based on the relationship between ( $C$ ), ( $\log C$ ), and the aquifer vulnerability index ( $AVI$ ) indicated in Table 1 (Stempvoort et al., 1993), the thirty-four  $VES$  locations in the Khanasser area are classified as follows ( [Table 2](#)):

The rating of (*AVI*) is exceptionally high in the *VES* (V2-5 and V9-1).

The rating of (*AVI*) is high in the *VES* (V9-3, Sh13, V8-3, V3-1, V3-2, V7-2, V7-3, V3-5, V5-4, V10-4, V10-1, V9-2, V9-4, V8-2, V5-3, V5-5, V4-3, V3-3, V3-4, V2-2, V2-3, V2-4, and V1-2).

The rating of (*AVI*) is moderate in the *VES* (V2-2, Sh11, Sh12, V6-2, V10-3, V10-2, V6-3, and V2-1).

The rating of (*AVI*) is low in the *VES* (V6-1).

The overburden protective capacity (*OPC*) of the aquifer Quaternary in the study area has been already modeled by applying the following equation (Asfahani, 2023a; Asfahani, 2023b):

$$OPC (\Omega^{-1}) = \sum_{i=1}^n \frac{h_i}{\rho_i} = \frac{h_1}{\rho_1} + \frac{h_2}{\rho_2} + \dots + \frac{h_n}{\rho_n} \quad (9)$$

where  $\rho_i$  is the resistivity and  $h_i$  is thickness of each covering layer.

It has been indicated, according to the classification of Heinret (1976), that as much the longitudinal conductance ( $\Omega^{-1}$ ) of the overburden protecting layers is bigger, as much the *OPC* is bigger (Asfahani, 2023a).

Fig.14 shows a good positive concordance between the results of both (*OPC*) and *AVI* techniques, where the correlation coefficient  $R^2$  of 0.60 is obtained for them. The equation between *OPC* and *Log C* has the following form:

$$\log C = 0.270 * \ln(OPC) + 2.267 \quad (R^2 = 0.60) \quad (10)$$

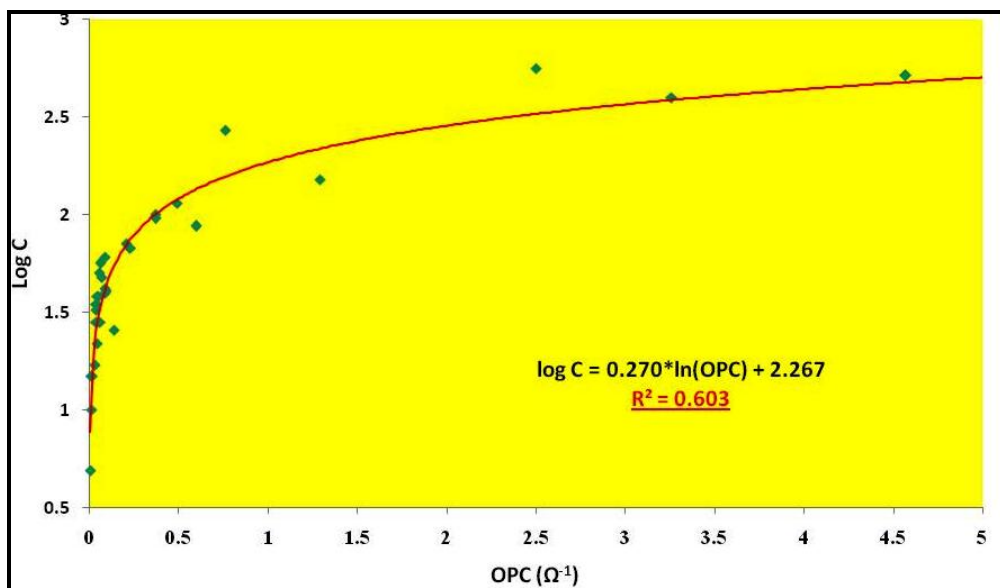


**Figure 14.** Empirical regression relationship between *OPC* and *Log C* in the study area.

The correlation matrix indicated in Table 3 shows the different relationships between (*log C*), and the thickness, resistivity, hydraulic conductivity, anisotropy ( $\lambda$ ), and (*OPC*) of the overburden layers.

**Table 3.** Correlation matrix between the *hOverb*,  $\rho$ *Overb*, *K*,  $\lambda$ , *OPC* and (*Log C*) in the study area.

Variables	$\rho$ <i>Overb</i>	$\lambda$	<i>Log C</i>	<i>OPC</i>	<i>hOverb</i>	<i>K</i>
$\rho$ <i>Overb</i>	1	0.44	<u>-0.75</u>	-0.21	-0.21	0.48
$\lambda$		1	-0.16	0.08	0.15	0.1
<i>Log C</i>			1	0.35	0.56	-0.34
<i>OPC</i>				1	0.47	-0.09
<i>hOverb</i>					1	-0.082
<i>K</i>						1

An acceptable correlation is shown in Table 3 between *hOverb* and *Log C* (0.56), overburden resistivity and *Log C* (-0.75), and *K* and *Log C* (-0.34). Table 4 summarizes the statistical results of the different treated parameters related to the measured thirty-four *VES* points in the study area.

**Table 4.** Statistical results of the treated geoelectrical parameters in the study region.

Statis	<i>hOverb</i> ( <i>m</i> )	$\rho$ <i>Overb</i> ( $\Omega.m$ )	<i>K</i> ( <i>m/day</i> )	<i>C</i> ( <i>day</i> )	<i>Log C</i>	<i>OPC</i> ( $\Omega^{-1}$ )	$\lambda$
<b>Min</b>	1.1	1.5	0.002	0.55	-0.26	0.006	0.72
<b>Max</b>	28.9	539	32.64	1659.59	3.22	13.75	2.31
<b>AV</b>	5.33	64	1.59	146.68	1.74	0.87	1.24

<b>SD</b>	6.1	95	6.37	299.88	0.63	2.49	0.29
-----------	-----	----	------	--------	------	------	------

This paper discuss the influence of those different parameters in affecting the protectivity of the aquifer Quaternary from the fluid contaminations originated in the study area. The different geoelectrical results thus obtained in this paper are important and help the decision makers for locating the effective protected groundwater area in the study region.

## 6. Conclusion

The aquifer vulnerability index (*AVI*) methodology with using the (*VES*) technique is undertaken to assess the aquifer Quaternary protectivity in the semi-arid Khanasser Valley region of northern Syria. The inversion WINRESIST computer software program is used to quantitatively interpret the measured thirty-four *VES* points in terms of *ID* structure, to obtain the final geoelectrical inverted optimized models for the treated *VES* points. The different geoelectrical parameters and their influences on the aquifer protectivity and contamination conditions are well determined. This work also discusses the effects of the geoelectrical parameters controlling the overburden protective capacity of the aquifer Quaternary by analyzing the results obtained by the *AVI* approach with its related *Log C*. Those parameters are the thickness (*hOver*), the resistivity (*ρOver*), the hydraulic conductivity (*K*) of the overburden protecting layers, and the anisotropy of the subsurface hydrogeological layers (*λ*). It is found that as the layers covering the aquifer are thinner, and their hydraulic conductivities are higher, the aquifer will be increasingly vulnerable to pollution. The correlation matrix of the geoelectrical parameters with the different mutual empirical equations already established clearly indicate the considerable influence of those parameters (*hOver*, *ρOver*, *K*, and *λ*) on the spatial distribution of the *Log C* in the study region. The derived empirical relationships between the different analyzed hydro-geophysical parameters are essential to understand both the mutual hydrological processes and the lithological connectivity nature between the study aquifer Quaternary and its overlaying layers. This paper provides useful geoelectrical information, which help in locating the effective protected groundwater area in the semi-arid Khanasser Valley region in Syria. The results obtained in this paper allow decision makers to assess management scenarios and coordinate surface and groundwater resources effectively.

As such, the *VES* technique with the *AVI* methodology developed in this article helps the decision-makers for locating the polluted and protected aquifer zones.

It can be practiced successfully to characterize other similar hydro-geological context in Syria, and worldwide outside of the Khanasser region. The *AVI* approach as described above is practiced herein for the first time in Syria, and can be easily extended to cover and deal with other Syrian aquifers to determine their protectivity and contamination conditions. The *AVI* approach can be also applied worldwide to evaluate the protection conditions surrounding an aquifer in similar semi-arid regions.

### **7. Acknowledgment**

The author would like to thank General Director of the Syrian Atomic Energy Commission (SAEC), for permission to publish this research work. The German Ministry of Economic Cooperation and Development (*BMZ*) and the German Agency for Technical Cooperation (*GTZ*) are acknowledged for financial and administrative support to the Khanasser Valley Integrated Research Site (*KVIRS*) project. Professor. Late Rieser Armins (coordinator of the project) from Bonn University, Germany is deeply thanked for many useful discussions during the preparation stages of this project. Wilko Schweers, and Zuhair Masri from *ICARDA* are thanked for providing the logistic help during the realization of the geoelectrical measurements. Dr. Fares Asfari is cordially thanked for his many help at the different stages of the Khanasser project during his work at *SAEC*. *ICARDA* is highly thanked for providing the facilities and the logistics during the realization of the Khanasser Valley project. Cordial thanks and appreciation to all who participate efficiently in the Khanasser project. Cordial thanks for the anonymous reviewers for their remarks and suggestions that considerably improve the final version of this paper.

### **6. Funding**

This work is part of a scientific research “Khanasser Valley Integrated Research Site (*KVIRS*) project”, which is totally funded by the authority of the Atomic Energy Commission of Syria.

**7. Data availability** The datasets related to this research paper are available with the author; however, accessing these data or making them available to others upon a reasonable request requires special permission from the Syrian Atomic Energy Commission.

## 8. Declarations

Conflict of interest: The author declares that he has no known competing financial interests or personal relationships that could have appeared to influence the work reported in this.

## 9. References

- ACSAD., 1984**, Water resources map of the Arab countries. The Arab Center for the Studies of Arid Zones and Dry Lands, Damascus, Syria. ACSAD publication.
- Adeniji AE., Omonona OV., Obiora DN., Chukudebelu JU., 2014**, Evaluation of soil corrosivity and aquifer protective capacity using geoelectrical investigation in Bwari basement area; Abuja. *J Earth Syst Sci* 123:491–502.
- Asfahani J., 2007**, Geoelectrical investigation for characterizing the hydrogeological conditions in semi-arid region in Khanasser valley, Syria. *Journal of Arid Environments* 68 31–52.
- Asfahani J., 2023a**, Integrated geoelectrical investigation for characterizing the shallow Quaternary aquifer parameters, and its vulnerability to contamination: a case study from Semi-arid Khanasser Valley Region, Syria. *Water Practice & Technology* Vol 18 No 7, 1639 doi: 10.2166/wpt.2023.084.
- Asfahani J., 2023b**, The influence of hydro-geoelectrical parameters on the Quaternary aquifer and its protectivity and contamination: a case study from Khanasser Valley Region, Northern Syria. *Water Practice & Technology* Vol 18 No 12, 3235 doi: 10.2166/wpt.2023.212.
- Ayuk MA., 2019**, Groundwater aquifer vulnerability assessment using a Dar-Zarrouk parameter in a proposed aboru residential Estate, Lagos State, Nigeria. *J Appl Sci Environ Manag* 23(12):2081–2090.
- Dobrin MB., 1988**, Introduction to geophysical prospecting, 4th edn. McGraw-Hill Book Company, New York.
- Ebong DE., Anthony EA Anthony AO., 2014**, Estimation of geohydraulic parameters from fractured shales and sandstone aquifers of Abi (Nigeria) using electrical resistivity and hydrogeologic measurements. *J Afr Earth Sci* 96:99–109. <https://doi.org/10.1016/j.jafrearsci.2014.03.026>.

**Ekanem AM., George NJ., Thomas JE., Nathaniel EU., 2020**, Empirical relations between aquifer geohydraulic—gEOelectric properties derived from surficial resistivity measurements in parts of Akwa Ibom State, Southern Nigeria. *Nat Resour Res* 29(4):2635–2646. <https://doi.org/10.1007/s11053-019-09606-1>.

**Ekanem AM., Akpan AE., George NJ., Thomas JE., 2021**, Appraisal of protectivity and corrosivity of surficial hydrogeological units via geo-sounding measurements. *Environ Monit Assess* 193:718. <https://doi.org/10.1007/s10661-021-09518-9>.

**Ekwe AC., Opara AI., Okeugo CG., 2020**, Determination of aquifer parameters from geo-sounding data in parts of Afikpo sub-basin southeastern Nigeria. *Arab J Geosci*. <https://doi.org/10.1007/s12517-020-5137-y>.

**Eyankware MO., 2019**, Integrated Landsat Imagery and Resistivity Methods in Evaluation of Groundwater Potential of Fractured Shale at Ejekwe Area, southeastern Nigeria, Unpublished PhD Thesis.

**Eyankware MO., Ogwah C., Selemo AO., 2020a**, Geoelectrical parameters for the estimation of groundwater potential in fracture aquifer at the sub-urban area of Abakaliki SE, Nigeria. *Int J Earth Sci Geophys*. <https://doi.org/10.35840/2631-5033/1831>

**Eyankware MO., Selemo AOI., Obasi PN., Nweke OM., 2020b**, Evaluation of groundwater vulnerability in fractured aquifer using geoelectric layer susceptibility index at Oju southern Benue Trough Nigeria. *Geol Behav* 4(2):63–67.

**Eyankware MO., Aleke G., 2021**, Geoelectric investigation to determine fracture zones and aquifer vulnerability in southern Benue Trough southeastern Nigeria. *Arab J Geosci*. <https://doi.org/10.1007/s12517-021-08542-w>.

**Eyankware MO., Akakuru CO., Eyankware EO., 2022**, Hydrogeophysical delineation of aquifer vulnerability in parts of Nkalagu areas of Abakaliki, SE. Nigeria. *Sustainable Water Res Manag*, <https://doi.org/10.1007/s40899-022-00603-6>.

**Henriet JP., 1976**, Direct application of the Dar Zarrouk parameters in groundwater surveys. *Geophys Prospect* 2:344–353. <https://doi.org/10.1111/j.1365-478.1976.tb00931.x>.

**Ibuot JC., George NJ., Okwesili AN., Obiora DN., 2019**, Investigation of lithotectonic characteristics of aquifer in Nkanu West local government area of Enugu state, Southern Nigeria. *Journal of African Earth Sciences*. 153, P. 197–207.

**IKpe EO., Ekanem AM., George NJ., 2022**, Modeling and assessing the protectivity of hydrogeological units using primary and secondary geoelectric indices: a case study of Ikot Ekpene Urban and its environs, southern Nigeria. *Modeling Earth Systems and Environment*. <https://doi.org/10.1007/s40808-022-01366-x>.

**Laouini G., Sunday EE., Okechukwu EA., 2017**, Delineation of aquifers using Dar Zarrouk parameters in parts of Akwa Ibom, Niger Delta. *Nigeria J Hydrogeol Hydrol Eng* 6(1):1–8. <https://doi.org/10.4172/2325-9647.1000151>.

**Mogaji KA., Omosuyi GO., Olayanju GM., 2011**, Groundwater system evaluation and protective capacity of overburden material at Ileoluji, Southwestern Nigeria. *J Geol Min Res* 3(11):294–304.

**Obiora ND., Ibuot CJ., 2020**, Geophysical assessment of aquifer vulnerability and management: a case study of University of Nigeria, Nsukka, Enugu State. *Applied Water Science*.;10(1):1–11. Available from: <https://dx.doi.org/10.1007/s13201-019-1113-7>.

**Obiora DN., Ibuot JC., George NJ., 2016**, Evaluation of aquifer potential, geoelectric and hydraulic parameters in Ezza North, southeastern Nigeria, using geoelectric sounding. *Int J Environ Sci Technol* 13:435–444. <https://doi.org/10.1007/s13762-015-0886-y>.

**Oli ICCA., Ahairakwem Opara., EkweOsi OkekeUrom., UdehEzennubia AIACIOOHMVC., 2020**, Hydrogeophysical assessment and protective capacity of groundwater resources in parts of Ezza and Ikwo areas, southeastern Nigeria. *Int J Energy Water Resour*. <https://doi.org/10.1007/s42108-020-00084-3>.

**Ossai MN., Okeke FN., Obiora DN., Ibuot JC., 2020**, Vulnerability assessment of hydrogeologic units in parts of Enugu North, Southeastern Nigeria, using integrated electrical resistivity methods. *Indian Journal of Science and Technology* 13(34): 3495–3509. <https://doi.org/10.17485/IJST/v13i34.1366>.

**Oseji JO., Egbai JC., Okolie EC., Ese EC., 2018**, Investigation of the aquifer protective capacity and groundwater quality around some open dumpsites in Sapele Delta State. Nigeria Hindawi Appl Environ Soil Sci. <https://doi.org/10.1155/2018/3653021>.

**Othman A., Beshr AM., Abd El-Gawad AMS., Ibraheem IM 2022**, Hydrogeophysical investigation using remote sensing and geoelectrical data in southeast Hiw, Qena, Egypt, Geocarto International, DOI: 10.1080/10106049.2022.2087750.

**Ponikarov., 1964**, The Geological Map of Syria, 1:200.000 and Explanatory Notes. Syrian Arab Republic, Ministry of Industry, Department of Geological and Mineral Research, Damascus, Syria.

**Singh KP., 2005**, Nonlinear estimation of aquifer parameters from surficial resistivity measurements. Hydrol. Earth Syst. Sci. Discuss. 2:917–923.

**Stempvoort DV., Ewert L., Wassenaar L., 1993**, Aquifer vulnerability index: a GIS—compatible method for groundwater vulnerability mapping. *Canadian Water Resources Journal.*;18(1):25–37. Available from: <https://dx.doi.org/10.4296/cwrj1801025>.

**Velpen BPA., Sporry RJ., 1993**, Resist: a computer program to process resistivity sounding data on PC compatibles. *Comput Geosci* 19(5):691–703.

**Zohdy AAR., 1989**, A new method for the automatic interpretation of Schlumberger and Wenner sounding curves. *Geophysics* 54, 245–253.

**Zohdy AAR., Bisdorf RJ., 1989**, Schlumberger Sounding Data Processing and Interpretation Program. U.S. Geological Survey, Denver.